Eletrônica de Potência
Open Journal of Power Electronics

Received April 24, 2024; accepted August 27, 2024; Date of publication September 04, 2024.
The review of this paper was arranged by Associate Editor Levy F. Costa and Editor-in-Chief Heverton A. Pereira.

Digital Object Identifier http://doi.org/10.18618/REP.e202429

Design and Autonomy Evaluation of a Power Supply for Long Range IoT Devices Using Magnetic Field Harvested Energy from High Current

Rafael da Silva Ferraz [1], Sóstenes Gutembergue M. Oliveira [1], Horacio Tertuliano dos S. Filho [1], Cláudio Bastos da Silva [1]

[1]Federal University of Parana – UFPR, Postgraduate Program in Electrical Engineering, Curitiba, PR, Brazil.

e-mail: rafaelferraz@ufpr.br; sgmoliveira92@gmail.com; tertuliano@ufpr.br; clbtx@uol.com.br.

ABSTRACT This study introduces a circuit designed to enhance energy conversion and storage, facilitating autonomous and sustainable operation from harvested magnetic energy in IoT devices. Through comprehensive experimentation and analysis, the circuit's performance and reliability were assessed, showcasing its potential to provide a dependable power supply to IoT networks. Furthermore, various scenarios with different operation cycles and component combinations were simulated to validate the circuit's potential. The findings indicate that integrating strategies such as energy redundancy using supercapacitors and magnetic field energy harvesting can be effective without the need for batteries or optimization circuits. The autonomy tests and predictions indicate that the system can go several days even without the total interruption on the energy source.

KEYWORDS IoT, Harvested Energy, Supercapacitor, Electronic Circuits, Magnetic Field, Performance Evaluation, Autonomy.

I. INTRODUCTION

The connectivity of devices is a crucial factor for fostering the generation of data, performing subsequent analysis and enabling data driven decision-making. Therefore, it contributes to enhancing the efficiency of algorithms and integrated networks. This attribute is based on the ability of machines to operate in an intelligent and intuitive manner, which constitutes the driving force behind the Internet of Things (IoT). In this perspective, IoT entails the conception of everyday objects or things that, through interconnection, acquire intelligence, awareness, and interactivity.

Intelligent physical objects are the "things" in IoT. They can be represented by various sensors, such as Global Positioning System (GPS) for positioning, proximity sensors, environmental parameter detection or even network connectivity in data transfer scenarios. There was a 9 % growth in the number of connected devices between the years 2020 and 2021, reaching a total of 12.3 billion by September 2021 [1]. Furthermore, there is a projection that the number of IoT connections will reach 27 billion worldwide by the year 2025.

Despite significant advances in embedded systems technologies, energy sources for IoT devices remain a challenge, particularly for those designed with a focus on high availability and reliability. Consistently within this context, batteries still represent one of the main energy sources for IoT devices. However, the maintenance process involving battery replacement, heating or recharging, along with the generated electronic waste, presents a significant disadvantage to their use. [2], [3]

One solution is to utilize alternative energy sources. They stand out for utilizing distinct methods from conventional ones, typically providing low power output. Some of the alternative sources of electrical energy generation include solar, wind, tidal, and magnetic energy [4].

In [5], a comprehensive study was conducted on various types of harvested energy, including solar, electromagnetic radiation, kinetic, and thermoelectric, to replace traditional sources such as batteries. Despite the conclusion that this type of energy shows promise, there has not yet been a satisfactory solution in terms of how to store the energy. In [6], the Radio Frequency (RF) was adopted as a source of harvested energy, and the conclusions were similar, highlighting that IoT devices powered by collected energy still cannot completely do away with the need for a secondary source.

Fig. 1, adapted from [7], comparatively illustrates the characteristics of the various existing energy harvesting techniques.

Although some alternative energy sources have low energy density, it is possible to significantly improve the efficiency of the energy harvesting process through the use of equipment and circuits specifically optimized for this purpose, such as in [8], [9].

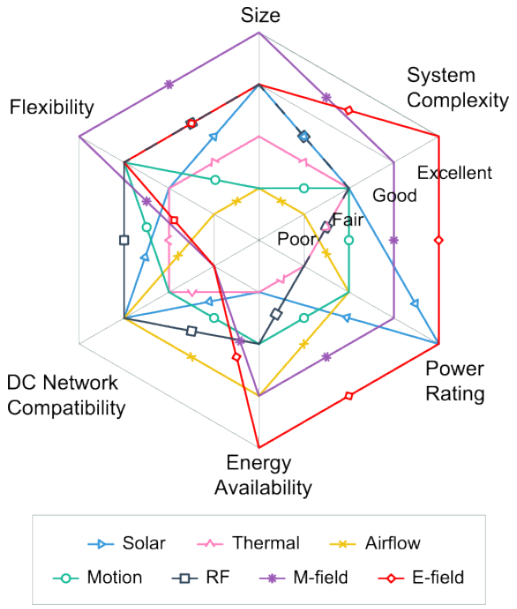

FIGURE 1. Comparison of Existing Energy Harvesting Techniques.

On the other hand, energy sources derived from magnetic fields are the most flexible and have considerably higher energy density compared to most other energy sources [7]. Additionally, another significant advantage lies in their specific characteristics, including the ability to be controlled and predicted, as it is not a natural variable in the environment, which happens in the case of solar energy, for instance.

Reference [10] built a hybrid energy harvesting system incorporating batteries and various sources of collected energy. They employ a Maximum Power Point Tracking (MPPT) system and voltage regulation methods through DC-DC converters. The authors' proposal is not to entirely replace the use of batteries, but rather to extend their lifespan. However, the use of MPPT implies the need of a system that requires more energy.

In [11], it was already presented the construction of a device that uses harvested magnetic energy to substitute battery. This work is an extension of that proposal, recapitulating the design and making an autonomy analysis for different scenarios in which the circuit could be applied and have its efficiency guaranteed.

II. HARVESTED ENERGY

Typically, the local power grid is used as the primary source for recharging the batteries of an IoT system, but this process incurs costs ranging from energy tariffs to labor for the personnel responsible for the recharging task.

Given this fact, alternative energy sources stand out by utilizing different sources than conventional ones, based on usually available energies, with the disadvantage of generally offering low power output.

The use of harvested energy in IoT systems presents the advantage of reducing the need for frequent battery replacement, which can be a challenge in applications with remote installations, such as rural or forested areas. In this context, energy harvested from magnetic fields are a good fit since it has the ability to operate in hostile environments, such as places with high temperatures or extreme pressures, isolated environments, or even underwater. These characteristics represent an attractive option for applications in industrial sectors, such as oil and gas exploration, mining, or in transmission lines.

Magnetic field harvesters are devices that capture and convert energy from the ambient magnetic field into usable power. These harvesters are designed to extract magnetic energy present in the environment and convert it into electricity, which can be used to power electronic devices. They consist of coils or antennas that are capable of capturing magnetic waves and converting them into electrical current. The harvested energy can be stored in batteries or used directly to power devices connected to the IoT network. Fig. 2 shows a diagram that illustrates the principle behind field harversters. [12]

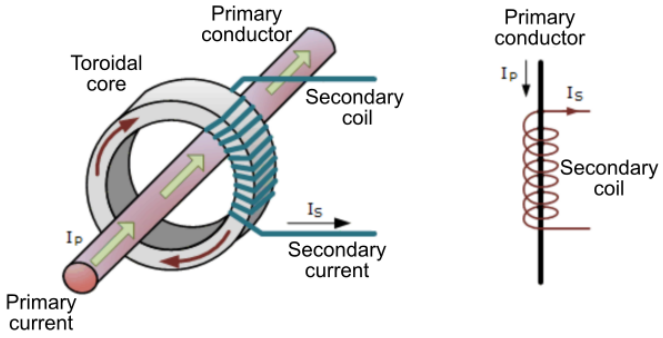

FIGURE 2. The operating principle of a field harvester (courtesy from [13]).

A. Emulating the Magnetic Field

For this work, we are going to create an adjustable magnetic field to be the primary power source of the designed circuit that will power the IoT device. In order to do so, we will use a commercial current transformer (CT). CTs are primarily used for electrical current measurement, protection, and control in high-power electrical systems.

The conceptual similarities between a magnetic field harvester for IoT applications and a commercial current transformer are factors that contribute to their utilization for the same purpose. In a current transformer, there are the primary and secondary windings that are magnetically coupled to transfer energy to measurement systems. In a magnetic field harvester, the coils are used to capture magnetic waves and convert them into usable electrical energy.

To enable the present study, an investigation of the power levels provided by the secondary side of a commercial current transformer and its ability to operate as a magnetic field harvester in energized conductors was conducted as a starting point. In [13], it was proven that smaller-sized CTs are unsuitable for the application at hand, as they fail

to provide the minimum voltage levels required for proper powering of IoT devices due to their internal voltage limiter, even when subjected to current levels close to their upper limits. Given this scenario, the decision was made to adopt a larger-sized CT, with current measurement capacities of 500 A.

The ZGCT $500A/5A$ CT 2.5 VA was selected. It is constructed with ABS polymer and has IEC60044-1 and ANSI c12.20 certifications. This model is categorized as split-core toroidal-shaped CTs made of ferrosilicon, a characteristic that facilitates installation. The 38 mm window size also contributes to this, as it allows for the passage of large gauge conductors.

To emulate a circuit that the harvest system will power, we are going to use a electronic load. It operates exclusively with direct current (DC), while the CT operates with both alternating current (AC) on the primary side and the secondary side. To overcome this issue, a full-wave bridge rectifier circuit and a capacitor were used to reduce signal ripple. This allows the root mean square (RMS) voltage to become equal to the peak-to-peak sinusoidal voltage, as the capacitor removes the pulsating DC value, as shown in Fig. 3.

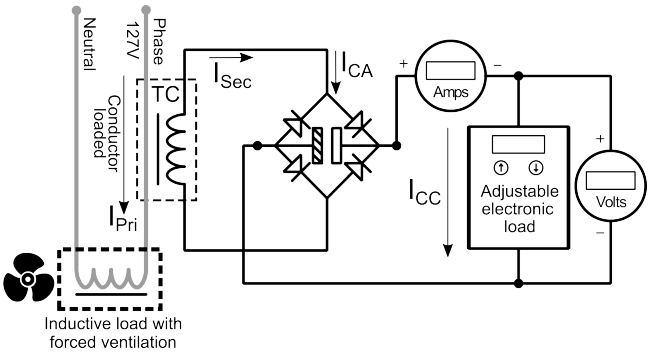

FIGURE 3. Electric Diagram of the test applied to the CT (from [11]).

To enable this operation, it was necessary to use an inductive load that would demand a reasonable level of current (6 A) on the primary side but would not exceed the levels of standard household outlets, which are approximately 10 A.

Considering that the selected CT has a full-scale range of 500 A, in order to generate current levels higher than 6 A, it was necessary to increase the number of wire turns passing through the toroidal window of the CT. Hence, only one turn means 6 A, whereas 10 turns represents 60 A theoretically. By adding more turns, the magnetic fields generated by the individual conductors are also effectively added, resulting in a higher overall current reading. Once the methodology to be applied to the primary of CT operating as a field collector had been defined, the electronic load was designed as shown in Fig. 4 (from [11]).

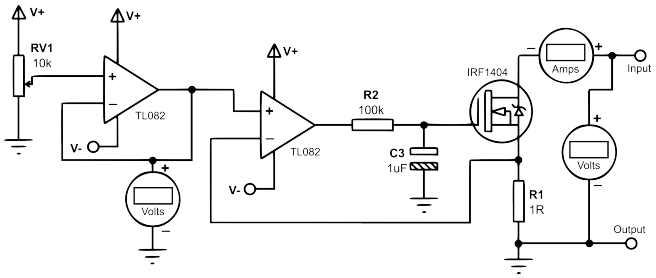

FIGURE 4. Electronic Load Circuit Diagram.

The operational amplifier used was the TL082, which is predominantly constructed using JFET (Junction Field Effect Transistor) inputs. This design feature provides it with a high input impedance of around 10^{12} Ω, a bandwidth of 4 MHz, and low noise levels.

B. Testing the Generated Magnetic Field

The power tests were conducted setting the current in the primary winding by adjusting the number of turns passing through the core window. This induces a stable magnetic field, thereby producing a proportional current in the secondary winding. Tests were performed gradually, changing the number of turns from 1 to 20. For the secondary, the test was conducted by varying the current demanded in steps of 50 mA until reaching a steady state.

The results of the test are shown in Fig. 5. The power generated by the secondary coil of the magnetic field collector is proportional to the field level resulting from the current passing through the conductor via the magnetic core.

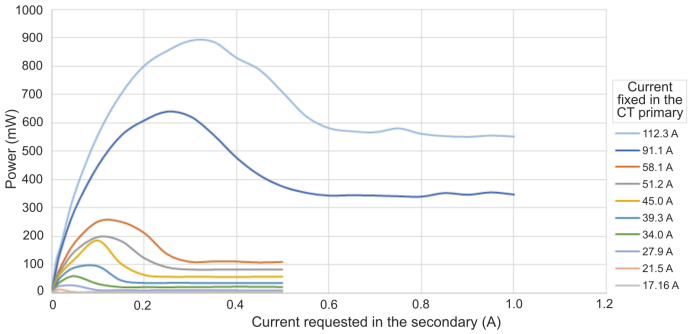

FIGURE 5. Power testing results.

This power also varies depending on the current demanded by the electronic load due to the characteristics of the maximum power transfer point, which, although relatively low, remains stable in steady-state regimes, being sufficient for use in Low Power electronic devices.

III. CIRCUIT DESIGN

The power source must be capable of adjustment for voltage and current levels from a harvested source to meet the requirements of the sensoring and control components, including the microcontroller.

A. Power Redundancy

To ensure the continuity of power supply in case of failures, the inclusion of power redundancy becomes necessary for the power source. A power supply system without redundancy can be easily disrupted by a failure in a critical component, which can lead to the shutdown of the equipment being powered. Fig. 6 illustrates the initial circuit concept of an energy redundancy system in the power source design, where the microcontroller represents the IoT device first connection.

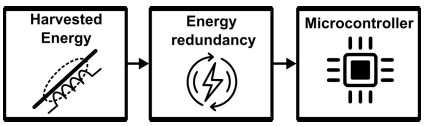

FIGURE 6. Power Supply Redundancy Flowchart.

Using supercapacitors is an approach to design such optimized circuits. Batteries and supercapacitors are distinct systems for electrical energy storage. For instance, lithium-ion batteries operate through chemical reactions involving cathodes and anodes immersed in a liquid electrolyte and separated by a micro porous separator permeable only to ions. On the other hand, supercapacitors store energy electrostatically. A supercapacitor utilizes a dielectric, an insulating material, between its plates to separate the positive and negative charges accumulated on each side of the plates [14]. Fig. 7 shows how supercapacitors compares to traditional Lithium batteries and other storage systems in terms of specificity.

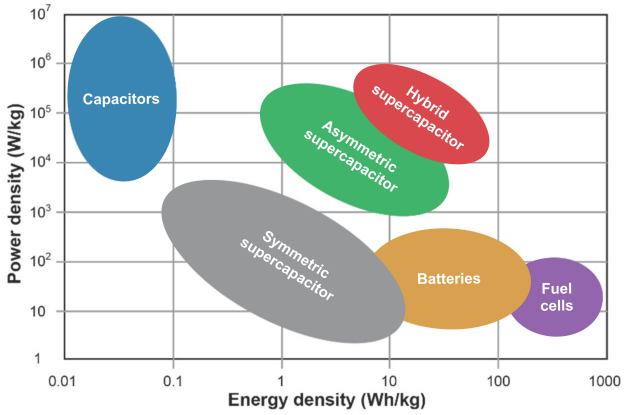

FIGURE 7. Plot of various energy storage devices (adapted from [15]).

In the past decade, global attention has turned to supercapacitors as a viable alternative to batteries. The main advantages of supercapacitors are their lightweight, compact size, long life cycle, rapid charge/discharge capability, high energy and power density, low cost, easy maintenance and absence of pollution.

This study examines supercapacitors as a battery alternative for the IoT application. A supercapacitor of $500\ F$ was used and it was tested using a electronic load. As expected, its voltage behavior was linear when demanded $500\ mA$. It is important to notice that this level of current is highly available through harvested systems, as mentioned in [16]–[18]. The charging time with $500\ mA$ using the electronic load was 23 minutes.

Using a electronic load on the supercapacitor, it was possible to generate the parameters presented in Table 1, and subsequently, calculating the Energy Density present in the supercapacitor, as shown in Table 2.

TABLE 1. Test results for a load of 500 mA in a 500 F capacitor.

Voltage Charg.(V)	Voltage Disch.(V)	Current (A)	Energy (Wh)	Capac. (mAh)	Weight (g)
≈ 2.7	0.6	0.5	0.3759	179	61.2

TABLE 2. Comparison between nominal and tested data in a 500 F capacitor.

Capacity (mAh)	Energy Calculated (Wh)	Energy Tested (Wh)	Density Ener. Calc. (Wh/kg)	Density Ener. Tested (Wh/kg)
179	0.50625	0.3759	8.272	6.142

B. Voltage Adjustments

If using batteries as energy redundancy, a series of management and control circuits are required. In general, discharging a Li-Po battery below $2.75\ V$ from its nominal voltage of $3.7\ V$ can already damage it. There are also safety issues such as temperature and even risks of explosions and fires.

To address this, battery banks need to have a BMS (Battery Management System), which is a dedicated technology for monitoring sets of battery cells, organized electrically in a row-by-column array configuration to deliver a specific range of voltage and current for a certain period.

On the other hand, for the use of supercapacitors in series configurations, only a few simple components are required to prevent them from being subjected to higher potential differences than their nominal operating value.

For this project, in order for it to be used in conjunction with a harvested power source and subsequently with a microcontroller, it is necessary to adjust the output and input voltages to meet the system specifications. The specific supercapacitor used, for instance, requires a charging voltage of $2.7\ V$ to reach its maximum capacity, while the microcontroller requires $3.3\ V$.

Fig. 8 includes the voltage adjustment modules between the harvested power and the supercapacitor, as well as between the supercapacitor and the microcontroller.

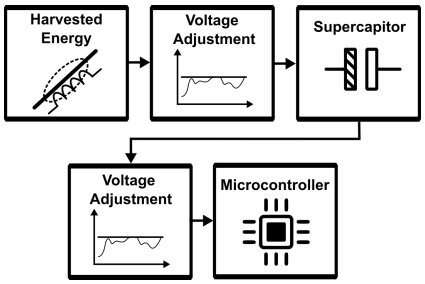

FIGURE 8. Power Supply Flowchart with Supercapacitor.

The first voltage adjustment module should handle the alternating current coming from the harvested magnetic energy source and ensure high efficiency in power transfer. The second module, in turn, should match the voltage of the supercapacitor to that of the microcontroller. Many works, such as [19], [20], use an additional circuit only for extracting the optimal power, but it demands even more from the source. Here, we are going to use a voltage multiplier.

1) Voltage multiplier

The AC output requires the use of a full-wave voltage doubler circuit. However, the output does not necessarily double the voltage when using common diodes with a current drain of $100\ mA$. This is mainly due to the voltage drop across the junction of common diodes, which is approximately $0.7\ V$. To reduce this voltage drop and achieve higher efficiency, the common diodes were replaced with Schottky diodes, specifically the 1N5822 model, which gives only a $0.3\ V$ drop.

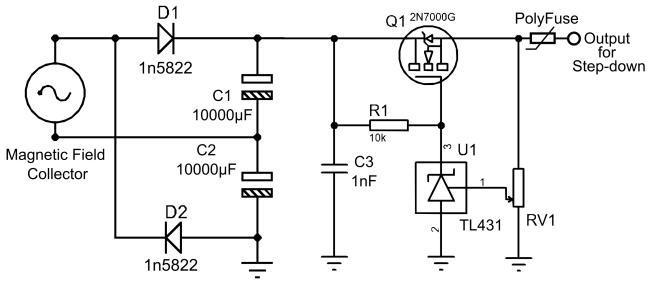

FIGURE 9. Voltage doubler, limiter voltage and current (from [11]).

Fig. 9 presents the circuit with adjusting steps of the voltage. First, there is the multiplier part with the diodes and the capacitors. Then, this output of the doubler circuit is limited by the subsequent components to ensure safe voltage levels for the rest of the circuit. This protection system is based on the TL431 integrated circuit. A potentiometer RV1 acts as an adjuster of the voltage levels and a transistor with higher power is utilized to act as the device that limits and dissipates energy, while the TL431 operates in a closed-loop configuration to maintain a stable output signal, preventing dangerous voltage spikes for subsequent devices [21].

A resettable polyfuse was also added in case of current surges and for thermal protection. It has the advantage of being reusable and resetting itself after a certain period of time, which reduces the need of human intervention and thus, maintenance costs.

2) DC-DC Converters

Supercapacitors provide their energy in a linear way, which could be a problem for embedded systems that commonly operate at voltages of $5\ V$ or $3.3\ V$. DC-DC converter circuits provide a solution, since they have the ability to convert one level of DC voltage to another, either stepping down or stepping up the signal.

Two converters were added: a step-down converter responsible for adjusting the voltage to power the supercapacitor and a step-up converter to adapt the voltage level for the microcontroller and the sensors integrated into the project.

The MP2307 chip from MPS was employed to build the step-down DC-DC converter. This chip offers high conversion efficiency, operating at $340\ kHz$, with a maximum input voltage of $23\ V$, adjustable output, a maximum current of $3\ A$, and a maximum power dissipation of $2\ W$.

Supposing a microcontroller that operates at $3.3\ V$, a voltage step-up circuit should be added. It is based on the ME2188 chip from Microne, which features high conversion efficiency, operating at $320\ kHz$, with an input range from $0.9\ V$ to $3\ V$. It provides a stable output of $3.3\ V$ and has a quiescent current of $7.5\ \mu A$.

Fig. 10 displays the result of a test with an electronic load ($100\ mA$) of the voltage signal at the output of the converter to verify the correct functioning of the device.

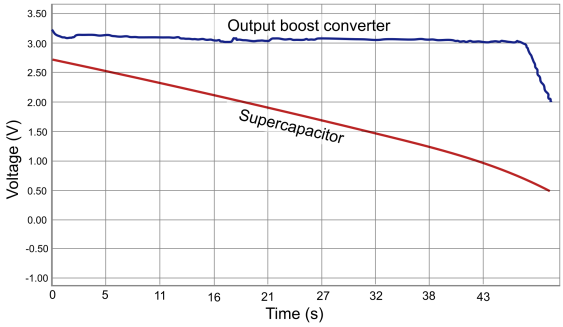

FIGURE 10. Result of the test on the voltage of the supercapacitor and the performance of the voltage step-up converter under a load of 100 mA.

Finally, in Fig. 11, we have the complete flowchart of the prototype with all the stages that were designed to optimize the circuit in terms of power (voltage doubler), safety (resetable fuse), redundancy (supercapacitor), and coherence (converters and limiters).

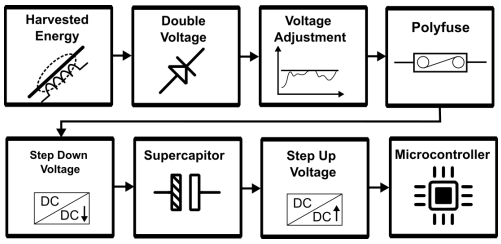

FIGURE 11. Block diagram detailing the entire constructed power supply.

Some works have achieved similar results building their circuits, but [22] used a power management unit instead of voltage doubler and [9] only had the project until the storage element.

IV. COMMUNICATION IN IOT

The Internet of Things is primarily based on a network of modules with unique identities that monitor specific variable values and transmit them to the internet through wireless communication. Some established technologies like RFID, Bluetooth, Wi-Fi, Zigbee, 3G, 4G, and 5G have been widely used within this concept. The inter connectivity present in the context of IoT inevitably leads to a considerable energy consumption, which demands the use of increasingly more efficient sources.

There is a direct relationship between the selected IoT network technology and the type of connectivity topology to be employed. Each one is designed to meet specific criteria, such as signal range, number of connected devices, density of information to be transported, data transmission interval, and energy consumption.

The constant advancement of microcontrollers and embedded systems has been crucial for the development of new connectivity technologies, gaining significant traction in IoT ecosystems. One of these breakthroughs was undoubtedly the LoRa (Long Range Radio) wireless communication technology. LoRa is known for its long-range and low-power functioning capabilities, has proven to be an efficient solution for applications involving energy harvesting systems due to its low energy consumption [23]. Fig. 12 shows the range comparison among the main wireless technologies available in the market.

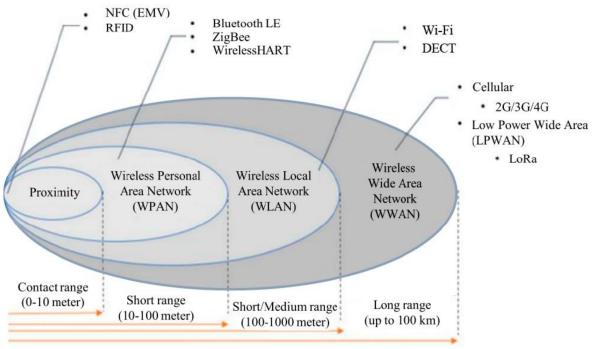

FIGURE 12. Signal range of selected wireless technologies (from [13]).

LoRa technology also provides a wide range of connectivity possibilities in energy harvesting systems. For instance, air quality monitoring sensors, temperature and humidity sensors, as well as tracking systems can be deployed in remote areas to collect data and transmit it to a control center [24].

V. POWERING IOT APPLICATIONS

Powering circuits in IoT involves unique considerations due to the diverse nature of its applications. IoT devices are typically designed to be energy-efficient, compact, and capable of operating autonomously for extended periods. Powering these circuits efficiently is critical to ensure reliable connectivity and functionality. Various powering strategies, ranging from steady-state to dynamic and irregular methods, are employed based on specific IoT requirements. Understanding these diverse approaches is essential for optimizing IoT device performance and energy consumption.

Powering sources for circuits operate in diverse ways depending on the application's needs. In steady-state conditions, a continuous and stable supply of power is delivered to the circuit, ensuring consistent performance. Alternatively, sources with active and inactive periods employ techniques similar to pulse-width modulation (PWM) to control power delivery intermittently. This method conserves energy and regulates circuit performance based on demand. In irregular scenarios, power sources adapt dynamically to varying requirements, adjusting voltage or frequency based on environmental or operational changes. This adaptability is crucial in renewable energy systems, where power generation fluctuates due to weather or system conditions. Fig. 13, from [25], illustrates the different types of energy provision.

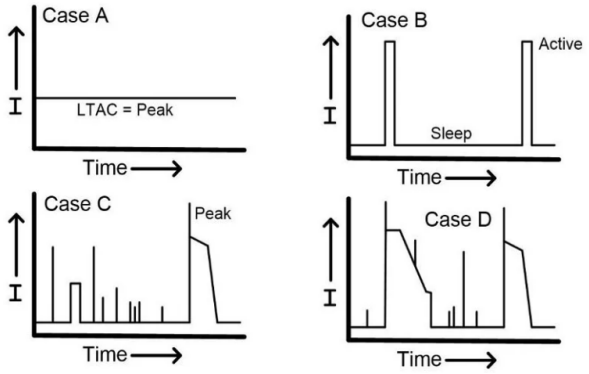

FIGURE 13. Four different power budget current profiles.

Considering Case B from Fig. 13 for our application, since the source of the magnetic field may not be constant, we can calculate the average current depending on the time spent in active mode and in sleep mode. Equation. 1 shows how to calculate it using weighted average:

$$I_{avg} = \frac{I_{active} * T_{active} + I_{sleep} * T_{sleep}}{T_{active} + T_{sleep}} \quad (1)$$

where I stands for current and T for time.

VI. SETS OF COMPONENTS

A. Microcontroller

One of the basic requirements for a device to be considered IoT is that it must have access to the internet. In the field of embedded systems, there are several possibilities for enabling cloud connectivity. Therefore, for this project, the versatile microcontroller from ESP32 family was chosen.

The ESP32-WROOM-32D chip model features a Dual-Core 32-bit Tensilica Xtensa LX6 processing core, with a clock speed of up to 240 MHz, as well as Wi-Fi and Bluetooth LE peripherals. This chip also has the ability to enter hibernation states, where it shuts down all unnecessary peripherals. In other words, once it completes its tasks, it goes to sleep for a predetermined period through programming, and only wakes up at defined intervals. Operating in light sleep, its consumption is approximately $0.8\ mA$, and in deep sleep, it is approximately $10\ \mu A$.

B. Sensors

An example application where diverse powering strategies are crucial could be within transmission lines, where abundant magnetic field energy is available for harvesting. In this context, it is important to have some key measurements for monitoring, such as temperature, humidity, smoke detection, and of course, current [26], [27].

We are going to create six different scenarios with sets of selected components to calculate the estimated demanded current, in order to verify if the supercapacitor can sustain the power. All of them combined with the ESP32, the ACS712 ($10\ mA$) for current measurement and the BME 680 ($12\ mA$) for Temperature. The whole circuit is operated at $3.3\ V$.

1) **Scenario 1**: LoRa 2.4Ghz - 500 mW for short range communication ($22\ mA$);
2) **Scenario 2**: LoRa 2.4Ghz - 500 mW for short range communication ($22mA$) and a smoke detector SCD4x ($175\ mA$);
3) **Scenario 3**: LoRa 915 Mhz - 500 mW for medium range communication ($230\ mA$);
4) **Scenario 4**: LoRa 915 Mhz - 500 mW for medium range communication ($230\ mA$) and a smoke detector SCD4x ($175\ mA$);
5) **Scenario 5**: LoRa 433 Mhz - 1 W for long range communication ($446\ mA$);
6) **Scenario 6**: LoRa 433 Mhz - 1 W for long range communication ($446\ mA$) and a smoke detector SCD4x ($175\ mA$).

Table 3 shows the total demanded current for each scenario described.

TABLE 3. Nominal demanded current from scenarios.

Scenario	Demanded Current (mA)
1	104
2	279
3	312
4	487
5	528
6	703

C. Autonomy

Now, with the different scenarios, we are going to simulate several cycles that will imply in different average currents. The operations cycles in which the calculations will be made are presented in Table 4. The active-sleep ratio refers to the operation shown in Fig. 13, case B.

TABLE 4. Cycle Operation.

Cycle Operation	Active-Sleep Ratio	Total Duration
CO1	1:7200	2h
CO2	1:3600	1h
CO3	1:1800	30 min
CO4	1:900	15 min
CO5	1:300	5min
CO6	1:60	1 min

From Table 2, we know that the energy supply capacity of the tested $500\ F$ supercapacitor is $1353.24\ Ws$. The entire operational cycle is going to vary according to Table 4, which includes microcontroller initialization, sensor data collection, and data transmission via the LoRa module. Dividing the total energy from the product of the voltage operation $3.3\ V$ and the average current calculated using (1), we obtain the autonomy in seconds. Dividing the result by 24 hours, we obtain the graph in Fig. 14.

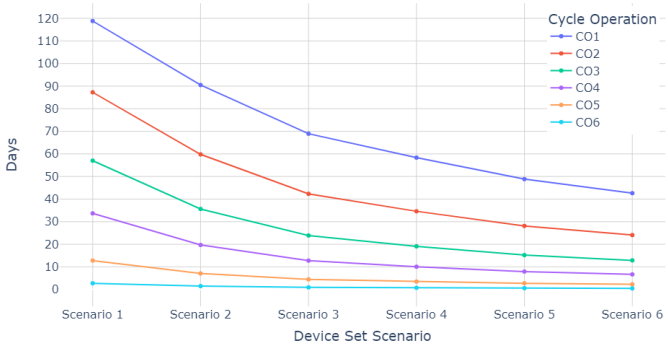

FIGURE 14. Autonomy (in days) per Scenario and Cycle Operation.

This result does not consider the self-discharge property of supercapacitors, being a result in a ideal scenario. According to [28], the self discharge can go up to 70% in a month,

therefore for a $3.3\ V$ maximum voltage which is the case for the $500\ F$ supercapacitor, it would go as low as $1\ V$ in an isolated scenario. However, the voltage step-up converter, as described in Fig. 9, maintains the same level of power for any level of voltage above $0.7\ V$. Hence, even in idle scenarios in which a break in the power source should happen, one could expect more than a month in autonomy for any of the scenarios presented in Fig. 14. Extreme conditions like variations in temperature may vary and interfere in the results as thoroughly discussed in [29].

D. Prototype Construction

Fig. 15 displays the IoT system implemented using the circuit as described in Scenario 1 previously with an enumeration for all of its parts.

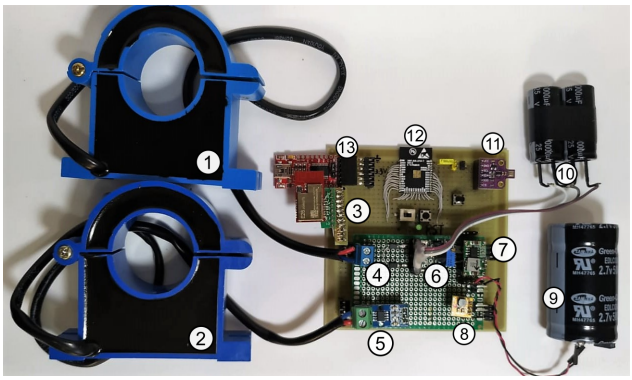

FIGURE 15. Final prototype.

Each component is described as follows:

1) Current transformer as field collector;
2) Current transformer as a current meter;
3) LoRa Module Ebyte E28-2G4M27S - The prototype can be used with various different LoRa modules. In the image, the Ebyte E28-2G4M27S is specifically shown. This module showed a great power efficiency in comparison to others in the market, as thoroughly tested in [13];
4) Voltage doubler circuit;
5) Hall effect sensor - This is the ACS712 sensor, which is based on the Hall effect and is designed to convert the current provided by the secondary of the CT into a proportional voltage. This is necessary because the ADC circuits of microcontrollers operate by measuring only low voltages;
6) Protection circuit;
7) DC-DC step-down Converter;
8) DC-DC step-up Converter;
9) $500\ F$ Supercapacitor;
10) Voltage doubler capacitor;
11) Environmental parameters sensor - This is the BME680 sensor from the manufacturer Bosch. It combines measurements of temperature, humidity, atmospheric pressure, and air quality in a single component. It operates at $3.3\ V$ and has low power consumption;
12) ESP32-WROOM-32D;
13) FTDI USB Converter - This board serves as an interface converter, enabling communication between the USB (Universal Serial Bus) standard and the $3.3\ V$ logic level UART (Universal Asynchronous Receiver/Transmitter) standard. These signals are essential for communication between a computer and the microcontroller. Hence, firmware updates are enabled and also facilitates the debugging process.

VII. DISCUSSION

The results shown in Fig. 14 demonstrate that there would be autonomy for the selected components for many days, even if the magnetic field from the source would be interrupted for many days. Even with a scenario with component that demanded more current and a high active period cycle, the supercapacitor fed by the collector could provide enough energy without recharging for almost half a day.

The work by [30] used supercapacitors as redundancy for systems with various types of harvested energy, including solar. The study concludes that, despite the search for circuits without conventional batteries, capacitors can assist in extending their lifespan.

In [10], it was developed an innovative architecture in which they collect energy from various sources to mitigate the low density issue in harvested energy systems. The combination of all these power sources is centralized in a supercapacitor.

In the research by [6], RF-collected energy is used, and a $50\ mF$ supercapacitor is used for redundancy. The recharge time was 2 minutes and 40 seconds, providing a fast utilization cycle compared to this work, which, due to discharge symmetry, would recharge in 23 minutes but offers much more energy.

VIII. CONCLUSION

By utilizing high-energy efficiency DC-DC circuits and incorporating supercapacitors, the batteries of the IoT device were completely replaced, enhancing its sustainability. Furthermore, the implementation of modern microcontrollers with deep sleep modes (ultra-low power consumption) was pivotal in achieving up several uninterrupted days of operation, even in extreme cases of total interruption of the magnetic field source and a high power demanding system.

This research successfully developed a self-sufficient IoT system with energy redundancy, voltage level adaptation circuits, and electrical protection, all powered entirely by magnetic fields. This includes the complete basic structure of an IoT system, encompassing sensors, microcontrollers, radio communication, and the construction of the source circuit utilizing a magnetic field produced in the laboratory.

IX. AUTHOR CONTRIBUTIONS

FERRAZ, R.S.: Conceptualization, Data Curation, Formal Analysis, Funding Acquisition, Investigation, Methodology, Project Administration, Resources, Software, Supervision, Validation, Visualization, Writing – Original Draft, Writing – Review & Editing. **OLIVEIRA, S.G.M.**: Data Curation, Formal Analysis, Software. **FILHO, H.T.S.**: Formal Analysis, Investigation, Supervision. **DA SILVA, C.B.**: Writing – Review & Editing.

PLAGIARISM POLICY

This article was submitted to the similarity system provided by Crossref and powered by iThenticate – Similarity Check.

REFERENCES

[1] S. Sinha, "State of IoT 2021: Number of connected IoT devices growing 9% to 12.3 billion globally, cellular IoT now surpassing 2 billion", *IoT Analytics: Market Insights for the Internet of Things*, 2021.

[2] A. Ostadi, M. Kazerani, "A comparative analysis of optimal sizing of battery-only, ultracapacitor-only, and battery–ultracapacitor hybrid energy storage systems for a city bus", *IEEE Transactions on Vehicular Technology*, vol. 64, no. 10, pp. 4449–4460, 2014, doi:10.1109/TVT.2014.2371912.

[3] M. Khalid, "A review on the selected applications of battery-supercapacitor hybrid energy storage systems for microgrids", *Energies*, vol. 12, no. 23, p. 4559, 2019, doi:10.3390/en12234559.

[4] J. M. Gilbert, F. Balouchi, "Comparison of energy harvesting systems for wireless sensor networks", *International Journal of automation and computing*, vol. 5, no. 4, pp. 334–347, 2008, doi:10.1007/s11633-008-0334-2.

[5] A. Michalski, Z. Watral, "Problems of powering end devices in wireless networks of the internet of things", *Energies*, vol. 14, no. 9, may 2021, doi:10.3390/en14092417.

[6] T. Sanislav, S. Zeadally, G. D. Mois, S. C. Folea, "Wireless energy harvesting: Empirical results and practical considerations for Internet of Things", *Journal of Network and Computer Applications*, vol. 121, pp. 149–158, nov 2018, doi:10.1016/j.jnca.2018.08.002.

[7] O. Cetinkaya, O. B. Akan, "Electric-field energy harvesting in wireless networks", *IEEE Wireless communications*, vol. 24, no. 2, pp. 34–41, 2017, doi:10.1109/MWC.2017.1600215.

[8] D. Monagle, E. Ponce, S. B. Leeb, "Generalized Analysis Method for Magnetic Energy Harvesters", *IEEE Transactions on Power Electronics*, vol. 37, no. 12, pp. 15764–15773, 2022, doi:10.1109/TPEL.2022.3195149.

[9] F. Yang, L. Du, H. Yu, P. Huang, "Magnetic and electric energy harvesting technologies in power grids: A review", *Sensors*, vol. 20, no. 5, p. 1496, 2020, doi:10.3390/s20051496.

[10] O. B. Akan, O. Cetinkaya, C. Koca, M. Ozger, "Internet of Hybrid Energy Harvesting Things", *IEEE Internet of Things Journal*, vol. 5, no. 2, pp. 736–746, apr 2018, doi:10.1109/JIOT.2017.2742663.

[11] R. D. S. Ferraz, S. G. Oliveira, H. Tertuliano Filho, C. B. Da Silva, "Power Supply Design for IoT Devices Using Magnetic Field Harvested Energy", *in 2023 IEEE 8th Southern Power Electronics Conference (SPEC)*, pp. 1–7, 2023, doi:10.1109/SPEC56436.2023.10408109.

[12] K.-S. Chang, S.-M. Kang, K.-J. Park, S.-H. Shin, H.-S. Kim, H.-S. Kim, "Electric field energy harvesting powered wireless sensors for smart grid", *Journal of Electrical Engineering and Technology*, vol. 7, no. 1, pp. 75–80, 2012, doi:10.5370/JEET.2012.7.1.75.

[13] R. d. S. Ferraz, *Dispositivo IoT de baixo consumo e longo alcance alimentado por energia coletada de campos magnéticos provenientes de condutores carregados*, Ph.D. thesis, UFPR - Universidade Federal do Paraná, 2023.

[14] K. K. Kar, *Handbook of nanocomposite supercapacitor materials II*, vol. 302, Springer, 2020.

[15] M. Jayaraj, A. Antony, P. Subha, *Energy Harvesting and Storage: Fundamentals and Materials*, Springer Nature, 2022.

[16] M. Kabakulak, S. Arslan, "Design and Application of an Electromagnetic Energy Harvester for Wireless Sensor Network", *in 2020 International Conference on Electrical, Communication, and Computer Engineering (ICECCE)*, pp. 1–6, IEEE, 2020, doi:10.1109/ICECCE49384.2020.9179409.

[17] S. Yuan, Y. Huang, J. Zhou, Q. Xu, C. Song, G. Yuan, "A high-efficiency helical core for magnetic field energy harvesting", *IEEE Transactions on Power Electronics*, vol. 32, no. 7, pp. 5365–5376, 2016, doi:10.1109/TPEL.2016.2610323.

[18] S. D. Vivenza, M. F. Gomes, "Energia, geração distribuída e o princípio da segurança jurídica", *Research, Society and Development*, vol. 11, no. 1, pp. e2111123417–e2111123417, 2022, doi:10.33448/rsd-v11i1.23417.

[19] O. A. Saraereh, A. Alsaraira, I. Khan, B. J. Choi, "A hybrid energy harvesting design for on-body internet-of-things (IoT) networks", *Sensors (Switzerland)*, vol. 20, no. 2, jan 2020, doi:10.3390/s20020407.

[20] S. Kawar, S. Krishnan, K. Abugharbieh, "Power Management for Energy Harvesting in IoT - A Brief Review of Requirements and Innovations", *in Midwest Symposium on Circuits and Systems*, vol. 2021-Augus, pp. 360–364, IEEE, aug 2021, doi:10.1109/MWSCAS47672.2021.9531846.

[21] S. Maniktala, *Switching power supply design & optimization*, McGraw-Hill Education, 2014.

[22] D. Vinko, "Power management circuit for energy harvesting applications with zero-power charging phase", *in 2017 40th International Convention on Information and Communication Technology, Electronics and Microelectronics (MIPRO)*, pp. 158–161, IEEE, 2017, doi:10.23919/MIPRO.2017.7973409.

[23] H. Gruber, "The evolution of market structure in semiconductors: the role of product standards", *Research Policy*, vol. 29, no. 6, pp. 725–740, 2000, doi:10.1016/S0048-7333(99)00046-3.

[24] J. M. Paredes-Parra, A. J. García-Sánchez, A. Mateo-Aroca, Á. Molina-García, "An alternative internet-of-things solution based on LOra for PV power plants: Data monitoring and management", *Energies*, vol. 12, no. 5, 2019, doi:10.3390/en12050881.

[25] J. Twomey, *Applied Embedded Electronics*, " O'Reilly Media, Inc.", 2023.

[26] A. H. Khawaja, Q. Huang, Z. H. Khan, "Monitoring of overhead transmission lines: a review from the perspective of contactless technologies", *Sensing and imaging*, vol. 18, pp. 1–18, 2017, doi:10.1007/s11220-017-0172-9.

[27] S. A. S. R. S. K. P. M. S. S. Abhinay Vijayrao Sahare, Shreyas Sunil Patil, "Transmission Line Fault Monitoring System Using IoT", *International Journal of Novel Research and Development (IJNRD)*, vol. 8, p. 5, 2023.

[28] J. Kowal, E. Avaroglu, F. Chamekh, A. Šenfelds, T. Thien, D. Wijaya, D. U. Sauer, "Detailed analysis of the self-discharge of supercapacitors", *Journal of Power Sources*, vol. 196, no. 1, pp. 573–579, 2011, doi:https://doi.org/10.1016/j.jpowsour.2009.12.028, URL: https://www.sciencedirect.com/science/article/pii/S0378775309022897.

[29] D. U. Sauer, D. U. S. Julia, K. Julia, K. Avaroglu, "Detailed Analysis of the Self Discharge of Supercapacitors", *Institute for Power Electronics and Electrical Drives Slide*, vol. 11, p. 13, 2008.

[30] A. Pop-Vadean, P. P. Pop, T. Latinovic, C. Barz, C. Lung, "Harvesting energy an sustainable power source, replace batteries for powering WSN and devices on the IoT", *in IOP Conference Series: Materials Science and Engineering*, vol. 200, Institute of Physics Publishing, may 2017, doi:10.1088/1757-899X/200/1/012043.

BIOGRAPHIES

Rafael da Silva Ferraz Currently pursuing a postdoctoral fellowship in Electrical Engineering at the Federal University of Paraná. Holds a Ph.D. in Electrical Engineering from the Federal University of Paraná (2023), a Master's degree in Electrical and Computer Engineering from the Federal University of Goiás (2016), a Bachelor's degree in Computer Network Technology from the Unified Higher Education Institute Objetivo (2012), and a Technical degree in Electrotechnics from the Federal Institute of Education, Science and Technology of Goiás (2014). Received postgraduate scholarships during the master's and doctoral programs, actively participat-

ing in various research groups. Has experience in Electrical and Electronic Engineering, with an emphasis on electronic prototyping and IoT.

Sóstenes Gutembergue M. Oliveira received the degree in control and automation engineering from the Federal Institute of Goias (IFG), having an Exchange Program with full scholarship in Western University (UWO) in London, Ontario. He achieved specialization in Data Science from the Technological Institute of Aeronautics (ITA). He has worked on researches by invitation and published papers with fellows from Federal University of Goias (UFG), Federal University of Parana (UFPR) and from Technological Federal University of Parana (UTFPR). He is currently a Data Scientist at Telefonica Brazil. Previous data scientist in the banking and agribusiness sector.

Horacio Tertuliano dos S. Filho received the degree in electrical engineering from the Federal Technological University of Paraná (UTFPR), with specialization from the University of Brasília, the master's degree from the University of Western Brittany, the Ph.D. degree from the University of Bordeaux I, and the Post-Ph.D. degree from the University of Montreal. All his trainings took place in telecommunications. He is currently a Full Professor with the Federal University of Paraná (UFPR), where he is currently the Dean of the School of Engineering. He is also the Director of the Telecommunications Laboratory (LabTelecomm), UFPR, where he has been directing several dissertations and doctoral thesis. His main area of interest includes transmission systems.

Cláudio Bastos da Silva Has a degree in electrical engineering, electronics, and telecommunications from the Federal Technological University of Paraná (UTFPR) and a master's degree from the Federal University of Paraná (UFPR) and is conducting his doctorate at UFPR. His main areas of interest include transmission systems, propagation, stochastic processes, and applied electromagnetism.